



# Design of experiment analysis on tensile properties of PLA samples produced by fused filament fabrication

Lionel Auffray<sup>1</sup> · Pierre-André Gouge<sup>2</sup> · Lamine Hattali<sup>1</sup>

Received: 23 June 2021 / Accepted: 10 October 2021 / Published online: 22 October 2021  
© The Author(s), under exclusive licence to Springer-Verlag London Ltd., part of Springer Nature 2021

## Abstract

The fused filament fabrication (FFF) is one of the most common forms of 3D printing with many hobbyists and as well as professional printers adopting this technology. With numerous printing parameters available for each print, having the knowledge to optimize the printing process to obtain a custom mechanical properties is clearly advantageous. This paper aims to analyze the elastic mechanical properties of PLA specimens manufactured through FFF process. To reduce experimental runs, the  $L_{27}$  Taguchi orthogonal array was used to analyze the influence of seven parameters, (i) infill pattern, (ii) layer height, (iii) infill density, (iv) printing velocity, (v) raster orientation, (vi) outline overlap, and (vii) extruder temperature, and three interactions, (i) infill pattern/layer height, (ii) infill pattern/infill density and, (iii) layer height/infill density on both Young's modulus ( $E$ ) and yield strength ( $R_{p0.2}$ ). To remove any doubt about certain parameters, a two-level fractional factorial design with four factors ( $2^{4-1}$ ) was used to supplement Taguchi approach. Results show that the infill density, infill pattern, printing velocity, and printing orientation are the most influential parameters, whereas layer height, extruder temperature, and outline overlap have no significant influence on Young's modulus and Yield strength. We show that the analysis of interactions could play a leading role in optimization parameters by removing doubt concerning some parameters. This work could be further developed to propose a model to help designers to obtain either tailor-made or a robust mechanical property with minimum variation and uncertainty in product.

**Keywords** Fused filament fabrication · Design of experiment · Taguchi's design · Fractional factorial design · Young's modulus · Yield strength · PLA

## 1 Introduction

Over the past few years, 3D printing, also known as additive manufacturing (AM), has become a topic of high interest from both academic and industrial sectors with increasing importance within the industry 4.0. This technology is defined as “a process of joining materials to make objects from 3D model data, usually layer upon layer” [1]. It was created to help the realization of what engineers have in

mind. Among the different available AM techniques such as stereolithography, selective laser melting (SLM), selective laser sintering (SLS), or laminated object manufacturing, to mention just a few, the fused deposition modeling (FDM<sup>TM</sup>) is the trendiest technique, although already existed since the 1980s. After the expiration of the Stratasys FDM<sup>TM</sup> patent in 2010, this technology is commonly known as fused filament fabrication (FFF). With a significant increase in sales, FDM<sup>TM</sup>/FFF printers are now the most prevalent 3D printer on the market. Nowadays, it is the technique showing the higher potential for product manufacturing, with the capability to compete with conventional polymer processing techniques [2]. Everyone knows that during COVID-19 pandemic, individuals, universities, research laboratories, and manufacturers have greatly participated in the development and manufacture of materials intended for health staff (facemasks, protective visor, or incubation tools). However, the mechanical performance of FDM<sup>TM</sup>/FFF 3D manufacturing process is governed by high number of parameters,

✉ Lamine Hattali  
lamine.hattali@universite-paris-saclay.fr

Lionel Auffray  
lionel.auffray@universite-paris-saclay.fr

Pierre-André Gouge  
pierre-andre.gouge@universite-paris-saclay.fr

<sup>1</sup> Université Paris-Saclay, CNRS, FAST, 91405 Orsay, France

<sup>2</sup> Université Paris-Saclay, IUT, 94234 Cachan, France

which are those that in any case must be controlled and defined to obtain optimum mechanical properties in the final pieces. These parameters also have a significant influence on other aspects of 3D-printed parts, such as dimensional accuracy, surface finish, or cost. So, the decision to take these and not other parameters could be difficult. Usually, operators choose these parameters under their experience and acquired knowledge, but there is not enough comprehensive information to determine suitable manufacturing parameters. Numerous studies and recommendations in the form of manuals or webpages have investigated the effects of some parameters which could potentially affect mechanical properties and fatigue life of 3D-printed parts [2–7]. The fishbone diagram provided in Fig. 1 highlights parameters that affect the mechanical properties and build time of print part based on the outcome of different existing studies since 2005.

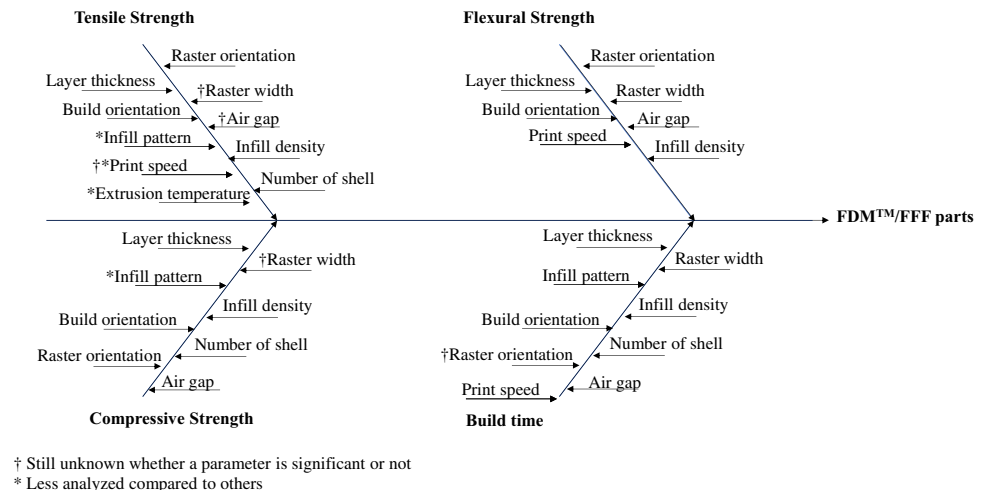
As observed in Fig. 1, the exploration of mechanical properties of samples obtained through FDM<sup>TM</sup>/FFF process has been extensively tackled with. Note that the most important parameters studied are (i) raster orientation, (ii) layer height/thickness, (iii) build orientation, (iv) infill density, (v) number of shell, (vi) gap between raster, and (vii) raster width. However, there are some process parameters such as infill pattern, print speed, or extrusion temperature which are less analyzed. And even when they are analyzed, the interaction effect with other parameters is not always tackled. It has been demonstrated that some parameters interacted with each other, making it both challenging to predict mechanical response of the material and critical to developing robust process-property relationships to aid the design. However, not all the FDM<sup>TM</sup>/FFF process parameters have the same impact on mechanical properties. In this context, remarkable experimental methods and designs of experiments were used to reduce the number of experimental runs and identify the best parameter combinations that improve mechanical

properties such as full factorial designs [8–10], Taguchi method [11–13], ANOVA [14], path planning strategies [15], automated neural networks search (ANS) [16–18], and fuzzy logic [19]. In these studies, a variety of processing parameters and their interaction effects were investigated at the same time.

Tensile strength is one of the most analyzed mechanical properties, and polylactic acid (PLA) is one of the widely used thermoplastics in FDM<sup>TM</sup>/FFF process. As noted from the reviewed studies [8, 20–23], build orientation has a more significant influence on mechanical properties than raster angle or orientation. Wang et al. [24] analyzed the impact of six parameters (layer thickness, deposition style, support style, build orientation and build location) on tensile strength. Their parts were built by an FDM machine (Stratasys P400 ABS). It was concluded that the sample printed in Z-direction (on-edge samples) was the most significant parameter for the tensile strength property. The build orientation was considered a variable to examine both quasi-static flexural and fatigue life by Terekhina et al. [23]. Regardless of the difficulty encountered to print PA6 thermoplastic, they showed that the sample printed in Z-direction (on-edge samples) present better static and dynamic mechanical properties.

Raster orientation was also studied in several references [25–28]. According to Letcher et al. [28], 0° raster orientation ensures the best tensile strength and elastic moduli. Tymrak et al. [29] confirmed this trend. They studied the effects of both layer and raster orientations, with three and two levels, respectively. Their findings were the average tensile strength and elastic modulus were higher for small layer heights and 0° raster orientation compared to 90° and ±45°. They also noted a large variability in the mechanical properties when using different 3D printers. Es-Said et al. [30] indicate that the ultimate and yield strength were the highest in the orientation where layers were deposited along the

**Fig. 1** A fishbone diagram to illustrate the main effect of process parameters on FDM<sup>TM</sup>/FFF part



length of the sample  $0^\circ$ , followed by those where the samples are built at  $\pm 45^\circ$  and  $90^\circ$ , respectively.

Another variable of the FDM printing process is printing speed or printing velocity. This parameter has influence in the process of melting and solidification of the filament. In addition, it affects the rate at which the molten polymer is extruded and deposited and then the quality of the printed parts. Setting a high printing speed can result in poor layer bonding and, hence, may lead to decrease the part's mechanical strength. Chacon et al. [31] studied the effect of layer thickness, print speed, and build orientation on the tensile strength. In the upright build orientation, an increase printing speed causes a measurable drop in tensile strength across all layer heights, whereas for the flat and on-edge samples, the printing speed appears to have minimal impact.

Another parameter with great influence is the layer height. Li et al. [32] studied and analyzed the layer height effect on the mechanical behavior of PLA samples. They conclude that tensile strength is better for small values of layer height. The same conclusions were mentioned for ABS, PLA, and PEEK [31, 32, 33, 34]. When the layer height was low, the contact surface is greater, and the free space between filaments is smaller; consequently the parts show a better cohesion between layers. The temperature also has a significant impact since it directly affects filament bonding. However, it was found that only few studies focus on its effect and interactions with other process parameters.

Behzadnasab and Yousefi [35] studied the influence of the set nozzle temperature of a PLA-3D printed part on the mechanical properties. The results show that the strength increased as the set nozzle temperature increased from 180 to 240 °C. Sun et al. [21] show that the envelope temperature and convective conditions influence the filament bonding and, thus, the tensile strength.

In the most cited studies, authors have adopted a 100% infill density for printed samples, whereas many practitioners will save time, cost, and materials and reduced the weight of parts by printing the samples at a reduced infill density and in some cases with different infill patterns [36,37,38]. Fernandes et al. [39] analyzed infill density, layer thickness, raster orientation, and extrusion temperature on mechanical tensile properties in the case of PLA. The optimum combination was high infill density and extrusion temperature, low layer thickness, and  $0^\circ/90^\circ$  raster orientation. Deng et al. [40] applied the Taguchi orthogonal array for experimental design and showed that a high print speed, low layer thickness, and high extrusion temperature were preferable for tensile strength. Using the same experimental design, the study of Rinanto et al. [41] revealed that a high extrusion temperature and infill density with a  $45^\circ$  raster orientation were optimum for tensile strength. Alafaghani et al. [42] examined the impact of six parameters on tensile mechanical properties: build orientation, infill density, infill patterns,

print speed, extrusion temperatures, and layer thickness. They used PLA as the filament and Makerbot Replicator 2X as the FFF machine. Among the six parameters, build orientation, layer thickness, infill density, and extrusion temperature were significant for tensile properties (Young's modulus, tensile strength, yield strength). Aw et al. [43] determined the impacts of infill density and infill pattern (rectilinear and line) on the tensile properties of both ABS/ZnO and ABS/ZnO built parts. Their study revealed that 100% infill density and a line infill pattern maximized tensile strength. Recently, Harpool et al. [44] evaluate the effect of infill pattern (rectangular, diamond, and hexagonal) on the tensile response of 3D-printed PLA. The infill percentage in each configuration is constant and equal to 15%. It was found that the pattern with hexagonal infill pattern has a higher ultimate tensile strength than all considered sample patterns.

This paper is focused on the study of both main and combined effects of FFF process on the elastic mechanical response of 3D PLA-printed specimens subjected to quasi-static tension load.

The novelty lies in the use both  $L_{27}$  Taguchi's approach and a two-level fractional factorial design. The interest of using these two approaches is to remove any doubt about certain parameters and their interactions. The purpose is twice: (i) deepen knowledge on the effect of parameters and their interactions and (ii) filling some gaps in the published literature, by taken into account the process parameters considered less analyzed. This approach permits to produce suitable datasets to aid designers choose and calibrate constitutive models for simulation of the response of 3D-printed parts.

The FFF process (Ultimaker 2) was used to print a batch of dog-bone-type specimen, for twenty-seven tensile tests for Taguchi analysis supplemented by eight tensile tests for fractional factorial analysis. For each manufacturing parameter set, five specimens were manufactured and tested, to evaluate both the apparent Young's modulus and the yield strength. The reason for choosing, in this study, to investigate PLA over other thermoplastics is primarily a practical one, since this material is very easy to print, and no warping phenomena was observed [38].

## 2 Experimental methods

In this section, the materials, equipment, and conditions used in the production and mechanical characterization of the samples are described in detail.

### 2.1 Material and specimen manufacture

The material used in this study for model fabrication is the thermoplastic filament Polylactide (EasyFil™ PLA)

produced by FormFutura® (Netherlands). Note that tensile modulus and tensile strength of filament are 3310 MPa and 110 MPa, respectively.

One big challenge with PLA filaments is that they absorb moisture from their surroundings. It is the moisture that the filament absorbs that produces fumes during printing and affects the quality of the printed specimen. To overcome this problem, the drying of the filaments before printing was carried out at 60 °C in vacuum oven for 6 h.

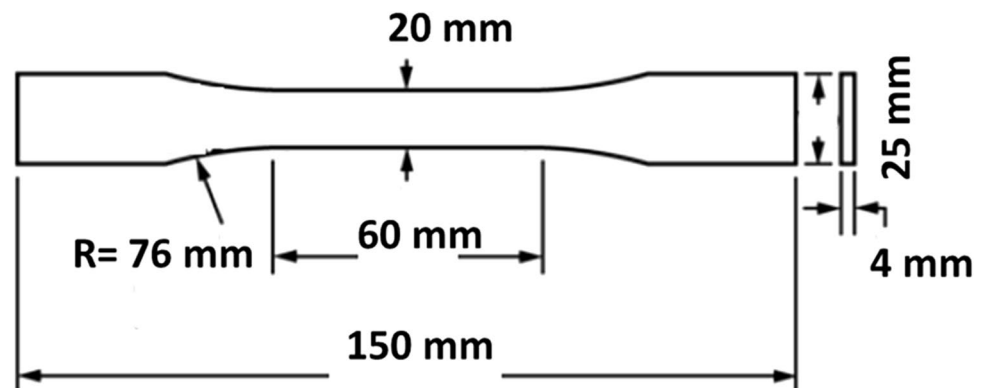
All the specimens were then stored in the dry atmosphere of a desiccator prior to testing. The specimens of FFF process were manufactured on the open-source Ultimaker 2 3D printer, Netherlands. The machine has the provision to vary all the seven chosen parameters.

## 2.2 Experimental set-up

The quasi-static tensile tests were carried out on the Instron 5852, electro-mechanical multi-space machine with a maximum load of 100kN. A 1 kN load cell was used to record the force under displacement-controlled condition at a constant rate of 100 mm/min. The constructed stress–strain figure for every specimen was used to extract both apparent Young's modulus ( $E$ ) and yield strength ( $R_{p0.2}$ ) from MATLAB routine (R2020b).

To date, no specific guidance is available to quantify the tensile strength of AM products, and most studies have referred to existing tensile strength test. The two key test standards that have been widely adopted are (i) ASTM D638 standard test method for tensile properties of plastics [45] and (ii) the equivalent ISO standard, BS EN ISO 527–2–1996 Plastics [46]. The principal drawback of using these standards in 3D printing materials is that in some case studies, the sample failure occurs at the bend radius, outside of the gauge length of the specimen due to stress concentrations. To overcome this issue, the bend radius was modified to minimize the stress concentrations. Figure 2 shows the geometry of the test specimens used. All specimens were printed using the same batch of PLA polymer.

**Fig. 2** The geometry of the test specimens used according to ASTM 638–14. The bend radius was modified to minimize the stress concentrations



## 2.3 Taguchi experimental design

After studying the literature reviews, it is found that the most influencing parameters on the quasi-static mechanical response of FFF parts are (i) infill pattern, (ii) layer height, (iii) infill density, (iv) printing velocity, (v) raster orientation (vi), outline overlap, and (vii) extruded temperature. Some parameters are more studied than others (see Fig. 1). These seven parameters were selected as factors for the experiment and serve as parameters for calculating the orthogonal arrays. Three levels for each factor were chosen as can be seen on Table 1.

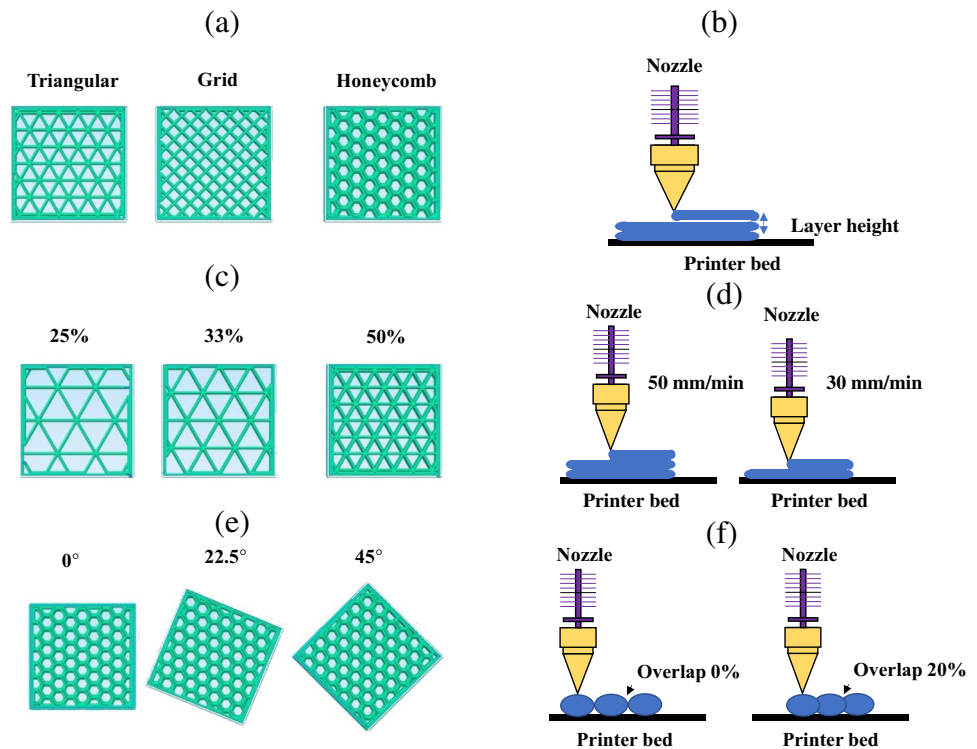
Therefore, the definitions of the FFF variable parameters in this study are as follows:

1. Infill pattern (F1): It defines the trajectories that the nozzle follows to fill the empty space within the contour (Fig. 3a). The choice of infill patterns (honeycomb, triangular, and grid) is motivated by their characteristics such as lightweight, high stiffness to weight ratio, and well-developed energy absorption. They are widely used in engineering.
2. Layer height (F2): It defines the thickness of each layer and, therefore, the number of layers the printed piece

**Table 1** Factors and control levels used for the design of experiments (DOE)

Parameters	Code	Level			Unit
		1	2	3	
Infill pattern	F1	Grid	Triangle	Honeycomb	-
Layer height	F2	0.1	0.15	0.2	mm
Infill density	F3	25	33	50	%
Printing speed	F4	1000	2000	3000	mm/min
Raster orientation	F5	0	22.5	45	°
Outline overlap	F6	10	20	30	%
Temperature	F7	205	210	215	°C

**Fig. 3** Schematic representation of the parameters used in the study: (a) infill pattern, (b) layer height, (c) infill density, (d) printing speed, (e) raster orientation, and (f) outline overlap



will have. It greatly affects the manufacturing time. Thinner layers imply more layers to print and a longer production time (Fig. 3b). The range of parameters variation (0.1, 0.15, and 0.2 mm) allows to obtain samples with a good surface quality.

3. Infill density (F3): It represents the amount of material that is deposited within the contours. It determines the distance between the inner threads and affects material consumption (Fig. 3c). The choice of parameters values (25%, 33%, and 50%) is motivated by our interest to printing lightweight materials.
4. Printing speed (F4): It represents the deposition of the filament velocity (Fig. 3d). The printing speed of 3000 mm/min is the maximum speed to obtain a samples with a good quality.
5. Raster orientation (F5): It denotes the angle at which the rods are laid during the construction of each layer during the FDM process, as detailed in (Fig. 3e).
6. Outline overlap (F6): It refers to the gap between adjacent raster tool paths on the same layer (Fig. 3f).
7. Temperature (F7): It defines the set nozzle temperature.

In classical methods of experimental planning a large number of experiments have to be carried out as the number of the process parameters increases, which is difficult and time-consuming and also results in higher cost. As an

example, if full factorial designs of experiment (DOE) is used, the study requires 729 ( $3^6$ ) experiments. To solve this problem, Taguchi [47] proposed an experimental plan in terms of orthogonal array that gives different combinations of parameters and their levels for each experiment. According to this technique, entire parameter space is studied with a minimum number of experiments. It is a powerful tool when a process is affected by a large number of parameters. In Taguchi design, selection of orthogonal array is an important issue for obtaining valid conclusions. Seven parameters, each at three level and three interactions, are considered in this study. The appropriate orthogonal array for this case is  $L_{27}$ . This array consists of 13 columns (C1, C2, ... C13) for assigning factors or interaction and 27 rows for designating the trials or experiment conditions (see Table 2). One the mechanical characterizations results were obtained, the statistical calculations were performed by the Minitab 18 software, and the interaction between the different parameters was analyzed. The average of each response characteristic for each level of each factor was analyzed based on Delta statistics, which compare the relative magnitude of effects. The Delta statistic is the highest minus the lowest average for each factor. Minitab assigns ranks based on delta values: rank 1 to the highest Delta value, rank 2 to the second highest, and so on.

**Table 2** Taguchi  $L_{27}$  orthogonal array design. This experimental planning has been performed, for each parameters, five times

N°	C1	C2	C3	C4	C5	C6	C7	C8	C9	C10	C11	C12	C13
	F1	F2	F1.F2	F1.F2	F3	F1.F3	F1.F3	F2.F3	F4	F5	F2.F3	F6	F7
1	1	1	1	1	1	1	1	1	1	1	1	1	1
2	1	1	1	1	2	2	2	2	2	2	2	2	2
3	1	1	1	1	3	3	3	3	3	3	3	3	3
4	1	2	2	2	1	1	1	2	2	2	3	3	3
5	1	2	2	2	2	2	2	3	3	3	1	1	1
6	1	2	2	2	3	3	3	1	1	1	2	2	2
7	1	3	3	3	1	1	1	3	3	3	2	2	2
8	1	3	3	3	2	2	2	1	1	1	3	3	3
9	1	3	3	3	3	3	3	2	2	2	1	1	1
10	2	1	2	3	1	2	3	1	2	3	1	2	3
11	2	1	2	3	2	3	1	2	3	1	2	3	1
12	2	1	2	3	3	1	2	3	1	2	3	1	2
13	2	2	3	1	1	2	3	2	3	1	3	1	2
14	2	2	3	1	2	3	1	3	1	2	1	2	3
15	2	2	3	1	3	1	2	1	2	3	2	3	1
16	2	3	1	2	1	2	3	3	1	2	2	3	1
17	2	3	1	2	2	3	1	1	2	3	3	1	2
18	2	3	1	2	3	1	2	2	3	1	1	2	3
19	3	1	3	2	1	3	2	1	3	2	1	3	2
20	3	1	3	2	2	1	3	2	1	3	2	1	3
21	3	1	3	2	3	2	1	3	2	1	3	2	1
22	3	2	1	3	1	3	2	2	1	3	3	2	1
23	3	2	1	3	2	1	3	3	2	1	1	3	2
24	3	2	1	3	3	2	1	1	3	2	2	1	3
25	3	3	2	1	1	3	2	3	2	1	2	1	3
26	3	3	2	1	2	1	3	1	3	2	3	2	1
27	3	3	2	1	3	2	1	2	1	3	1	3	2



## 3 Results and discussion

### 3.1 Application of Taguchi approach

In this section, the principal results relative to Taguchi analysis are fully described.

#### 3.1.1 Young's modulus and yield strength population characteristics

The apparent Young modulus of all the samples was done by finding the slope of a linear least-squares regression line in the elastic linear zone of stress versus strain curve. The maximum and minimum values obtained for apparent Young modulus of all the different permutations of the  $L_{27}$  array (population  $n = 135$ ) were 796 MPa and 248 MPa, respectively, with a mean value  $\mu = 487.8$  MPa (Fig. 4a).

As apparent Young modulus, the Yield strength ( $R_{p0.2}$ ) of all the samples was obtained by drawing a straight line through yield point at the same slope as the initial part of the stress–strain curve. The Yield strength values varies between 2.04 MPa and 9.49 MPa, with a mean value  $\mu = 5.76$  MPa (Fig. 4b). Note that both histograms illustrate that the data do not follow a normal distribution.

#### 3.1.2 Factor analysis for Young's modulus

To find the influence of the factors on apparent Young's modulus, the effect of factors on mean values as well as signal-to-noise (S/N) ratios for each factors were analyzed (Fig. 5).

The main effect for mean values of apparent Young modulus was calculated through Taguchi analysis yielded as a result that the (F3) infill density, (F1) infill pattern, (F4) printing speed, and (F5) printing orientation are the most influential factors from the greater to lesser. Using the cumulative delta of all the factors as a relative measure, it becomes that the two most significant factors are (F3) infill

density and (F1) infill pattern which contribute to ~36% and 29.2% of the response respectively followed by the printing speed (~13.6%) and printing orientation (~12.3%).

For the main factor (F3) infill density, it is noticeable that the influence is no linear, as the increase in apparent Young modulus is stronger when the part is filled from 33 to 50% of the nominal volume, in comparison to the improvement when increasing from 25 to 33%. The infill density results have a direct relation with the Young's modulus. Stiffness and yield strength increased in all structures with higher infill density. On the other side, elongations decreased with increasing infill densities. The decrease of elongation related to high infill density may be attributed to high defect density with more joining nodes [48]. The obtained results are perfectly consistent with literature [42, 43, 48, 49].

The (F1) infill pattern effect is mainly observed and was depending to (F5) print orientation and (F4) printing velocity. Triangular structure showed a higher influence on the result followed by grid and honeycomb structure for (F5) print orientation  $\pm 45^\circ$ . The samples with triangular infill structures were stiffer and less ductile than those filled with hexagonal and grid structures. This result was reported by Wang et al. [48] and was attributed to the beam theory. Similar experimental results were also observed by Lubombo et al. [49] in the perspective of elastic modulus. The triangle unit-filled PLA had a higher Young's modulus than that of the composites filled with hexagonal cells at a given infill density. For grid structure and for (F5) print orientation  $\pm 45^\circ$ , one can see that this orientation is corresponding to  $90^\circ/0^\circ$ , which aligns the filament direction with the axis of the tensile tests (Fig. 6). The results are consistent with those of fiber-reinforced composite where the best contribution is obtained when fibers are oriented in the axis for tensile testing.

However, it is evident that the cumulative effect of the four top ranked factors significantly outweighs the cumulative effects of the rest parameters. Note that the (F2) layer height, (F7) temperature, and (F6) outline overlap have

**Fig. 4** Young modulus and Yield strength characteristics: (a) histogram of the Young modulus population and (b) histogram of the yield strength population

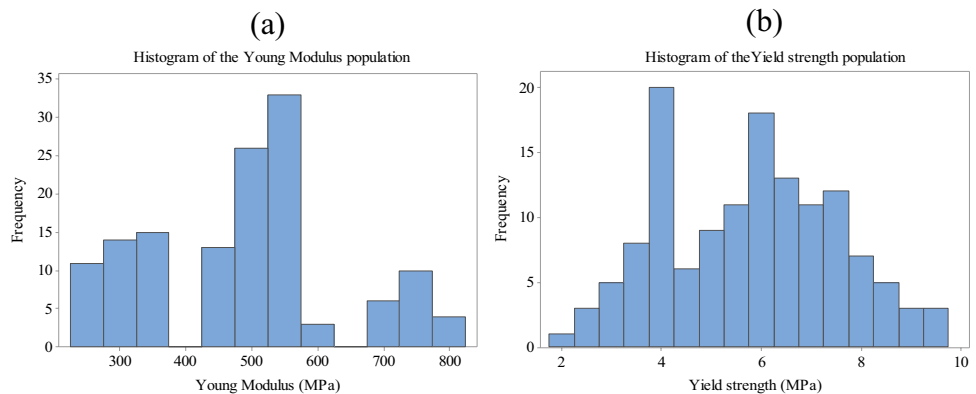
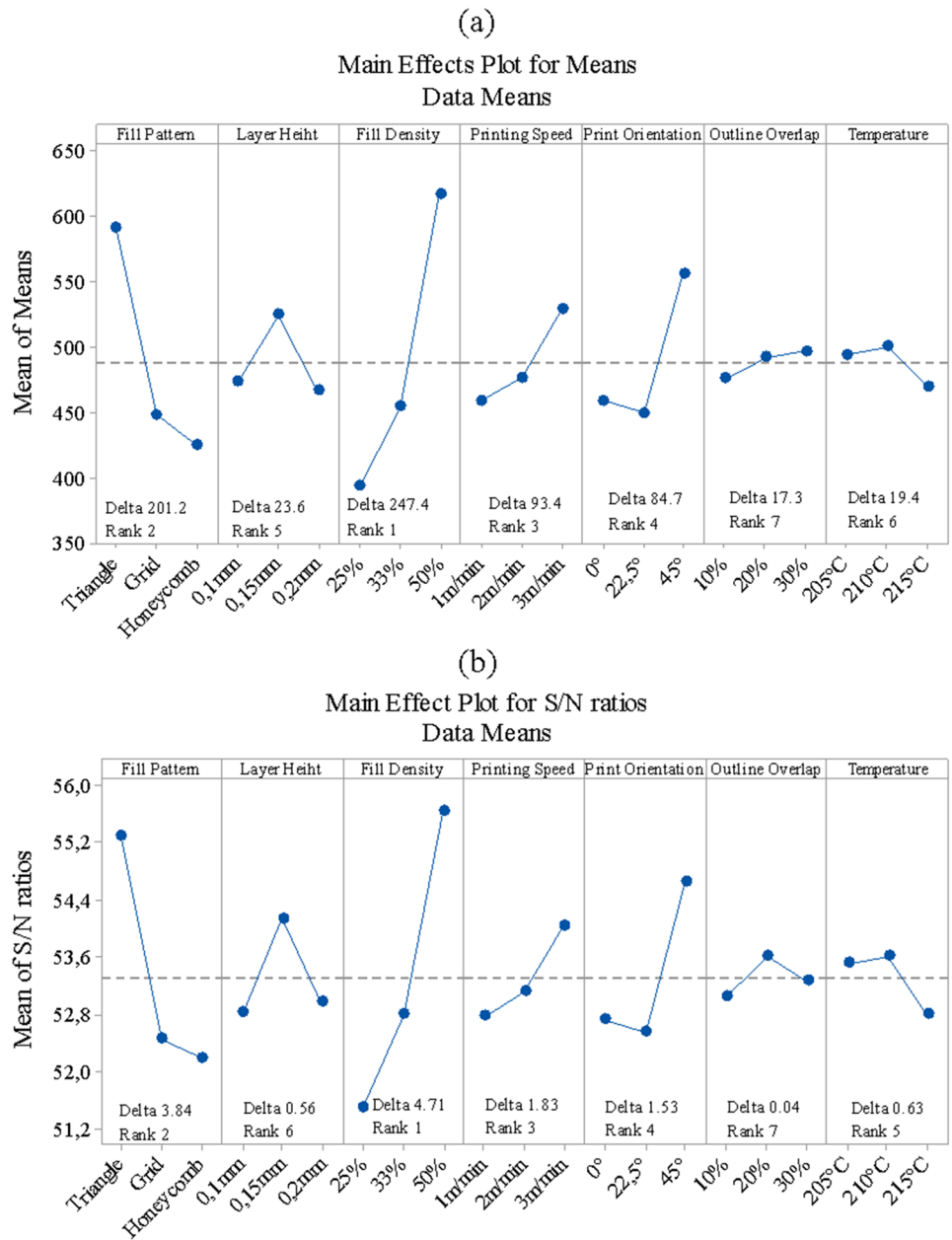
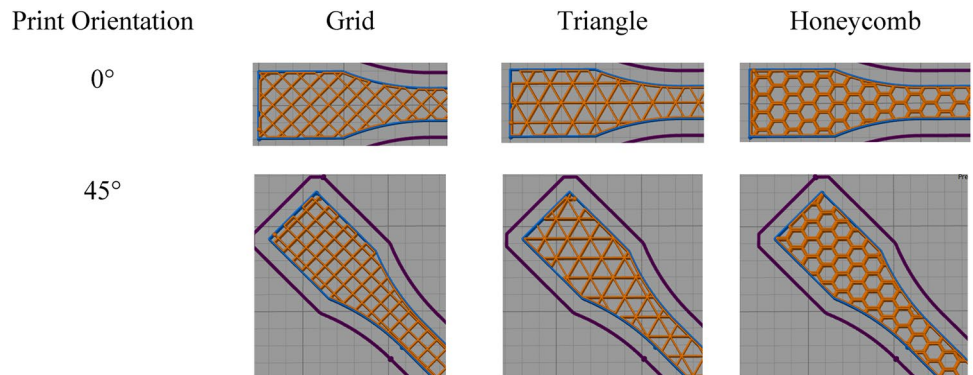


**Fig. 5** Main Effects Plot of Young modulus (MPa) obtained from Minitab: (a) for means values and (b) for signal-to-noise ratios (S/N)



Signal-to-noise: higher is better

**Fig. 6** Print orientation of the sample





extremely little or no significant effect on the Young’s modulus.

The value of apparent Young’s Modulus is transforming in S/N ratio values to find out the optimum combination of parameters for response variable. In our case, the “higher is better” is objective characteristic. The S/N ratios are calculated using the below mentioned formula:

$$S/N = -10\log\left(\frac{1}{N} \sum \left(\frac{1}{Y^2}\right)\right) \tag{1}$$

where Y is responses for the given factor level combination and n is the number of responses in the factor level combination.

These values of S/N ratio and averages will then further be analyzed to detect the most responsible factor and the percentage contribution of each factor on the maximization of Young’s modulus (response variable). Note that the analysis of signal-to-noise ratios shows a similar pattern to the graph of the main effect plot for means (see Fig. 5b).

The two most influential factors (F3) infill density (~36%) and (F1) infill pattern (29.2%) contribute to ~65% of the response in signal-to-noise ratio followed by the printing velocity (~14%) and printing orientation (~11.7%). However, the small difference, which has no consequence on

response, is observed in the classification of factors: (F7) temperature (~5%) and (F2) layer height (~4%) (Fig. 5b).

### 3.1.3 Interactions between the parameters

Interactions between infill pattern, layer height, and infill density were also assessed. Interaction plot for S/N ratio clearly indicates that there are no interactions between (i) infill pattern and layer height, and (ii) infill pattern and infill density. The interaction exists only between layer height and infill density. Previously, the main effect plots for S/N ratio (see Fig. 5b) give a preponderance of the effect of layer height of 0.15 mm (rank 6). Here, in all cases, the layer height of 0.1 mm maximizes the response with triangular infill pattern and infill density of 50% (Fig. 7). In this study, the analysis of interactions played a leading role. It is allowed to remove a doubt concerning the effect of layer height parameter which is considered without a significance effect.

From Figs. 5b and 7, it is concluded that the optimum combination of each process parameter for higher Young’s modulus is meeting at (F3) infill density, 50%; (F2) infill pattern, triangle; (F4) printing speed, 3 m/min; (F5) printing

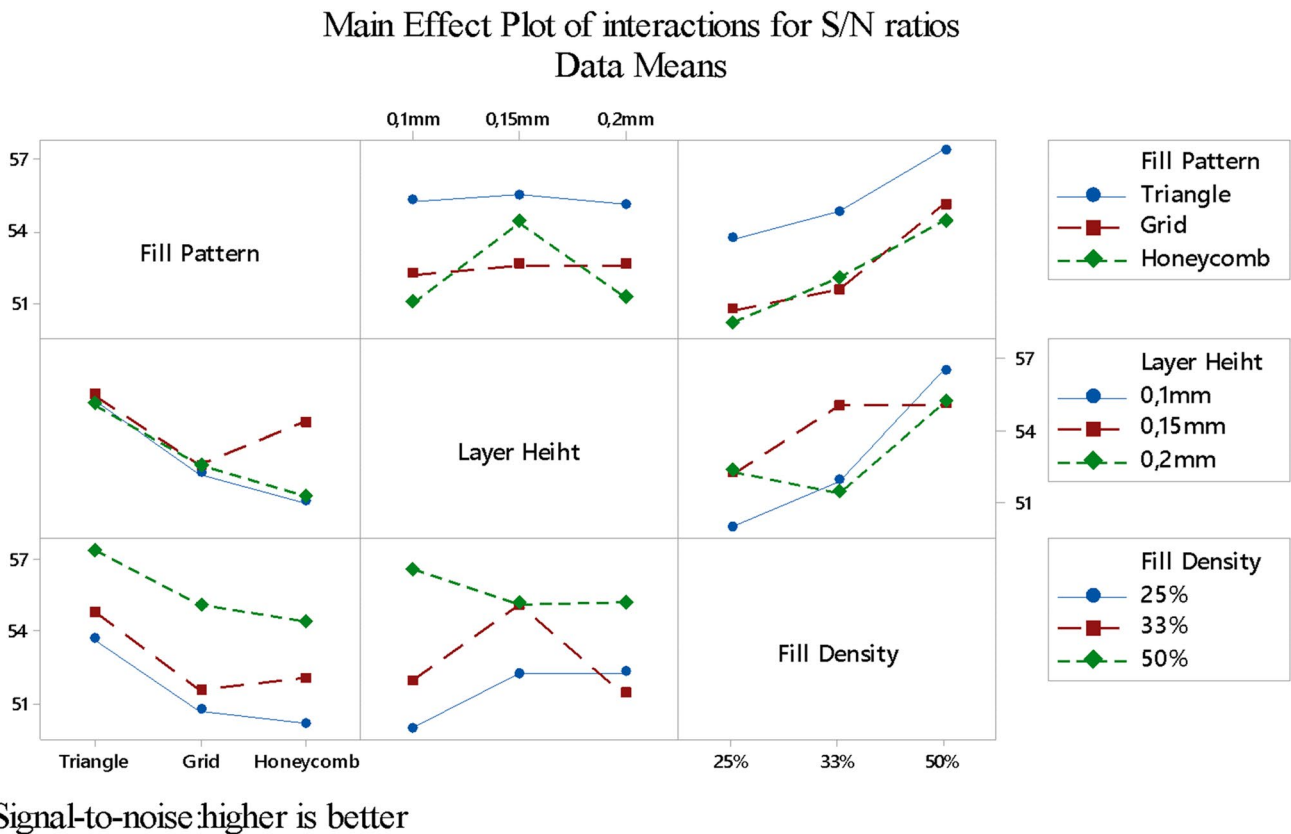


Fig. 7 Main effects plot for S/N ratios

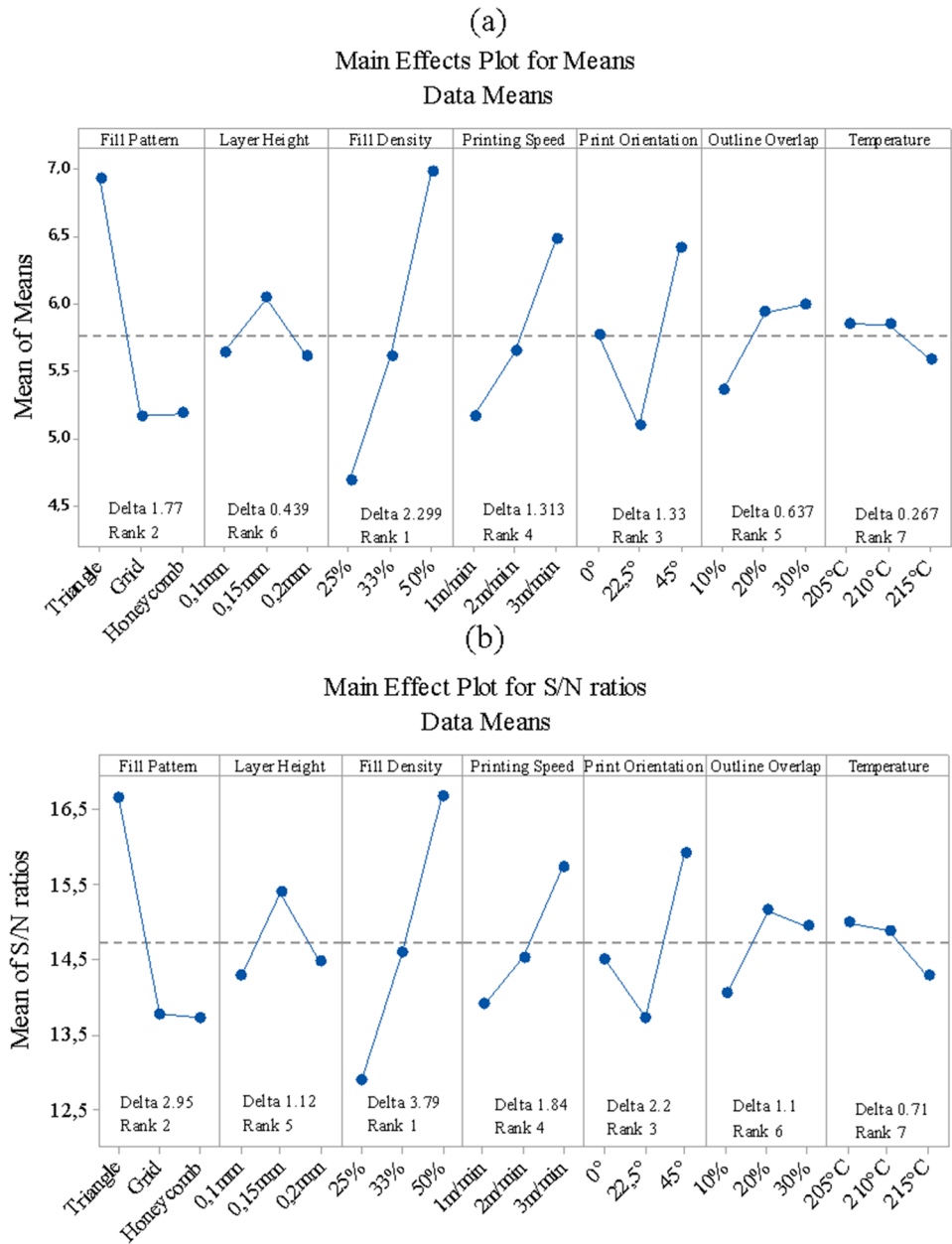
orientation, 45°; (F2) layer height, 0.1 mm; (F7) temperature, 210 °C; and (F6) outline overlap, 30%.

### 3.1.4 Factor analysis for yield strength

The same analysis was conducted to study the effects of the variation of the different factors on the yield strength, which is indicated in both graph on main effect plot for means and main effects plot for S/N ratios (Fig. 8a and b). The effect of the main parameters on the yield strength response follows the same pattern as in the case of Young’s modulus.

As for Young modulus analysis, there are no difference between the form of the signal-to-noise ratio (S/N) graphs and the graph of the means. The exploration experiment yielded as a result that the factors (F3) infill density, (F2) infill pattern, (F5) print orientation, and (F4) printing velocity are the most influential factor from greater to lesser mayor impact in yield strength, which each contribute to ~27.6%, 21.5%, 16%, and 13.4% of the response, respectively, whereas (F2) layer height (F6), outline overlap, and (F7) temperature seem to have a contribution smaller than 10% and considered as negligible effect. Note that for the main factor (F3) infill density, the influence is linear: when

**Fig. 8** Main Effects Plot of Yield strength obtained from Minitab: (a) for means values and (b) for signal to noise ratios (S/N)



Signal-to-noise: higher is better

the infill density increases from 33 to 50%, the yield strength increases from 4.69 to 6.98 MPa. The same observation was noted for (F4) printing velocity. Triangular infill pattern allows to obtain a higher yield strength especially when (F5) print orientation is  $\pm 45^\circ$ .

### 3.1.5 Interactions between the parameters

There is an interaction between the layer height and the infill density (Fig. 9). The maximum yield strength response is obtained for 50% infill density and layer height of 0.1 mm. From Figs. 8 to 9, the optimized values for obtained a maximum yield strength were (F3) infill density, 50%; (F1) infill pattern, Triangle; (F4) printing speed, 3 m/min; (F5) printing orientation,  $45^\circ$ ; (F2) layer height, 0.1 mm; (F7) temperature, 205 °C; and (F6) outline overlap, 20%.

### 3.2 Fractional factorial designs

To quantify the importance or not of some parameter’s effects and their interactions, a fractional factorial designs method was applied. Four parameters were selected for the study. Two of them significantly affect the behavior of material such as infill density and printing speed (see Figs. 5 and

8). The infill density is considered as main factor in both apparent Young modulus and Yield strength, whereas the printing velocity was considered as third most factors for Young modulus and fourth factor for Yield strength. For the remainder two parameters, i.e., temperature and layer height, the idea is to confirm their negligible both effect and interactions. The process parameters for which maximization is reached have been fixed (infill pattern, Triangle; print orientation,  $45^\circ$ ; and outline overlap, 30%). A two-level fractional factorial design with four factors ( $2^{4-1}$ ) was used. The four main parameters were (A) infill density, (B) velocity, (C) temperature, and (D) layer height, with three interactions: AB, AC, and AD (Table 3). The design requires eight runs per replicate. At least five specimens were tested for each configuration. The three- and four-factor interaction effects ABC and ABCD were neglected to evaluate both the Young’s modulus and yield strength.

Use the Pareto chart permit to determine the magnitude and the importance of the effects. The Pareto chart shows the absolute values of the standardized effects of both Young’s modulus and yield strength from the largest effect to the smallest effect (Fig. 10a and b).

It can determine which effects increase the response. The standardized effects are t-statistics that test the null

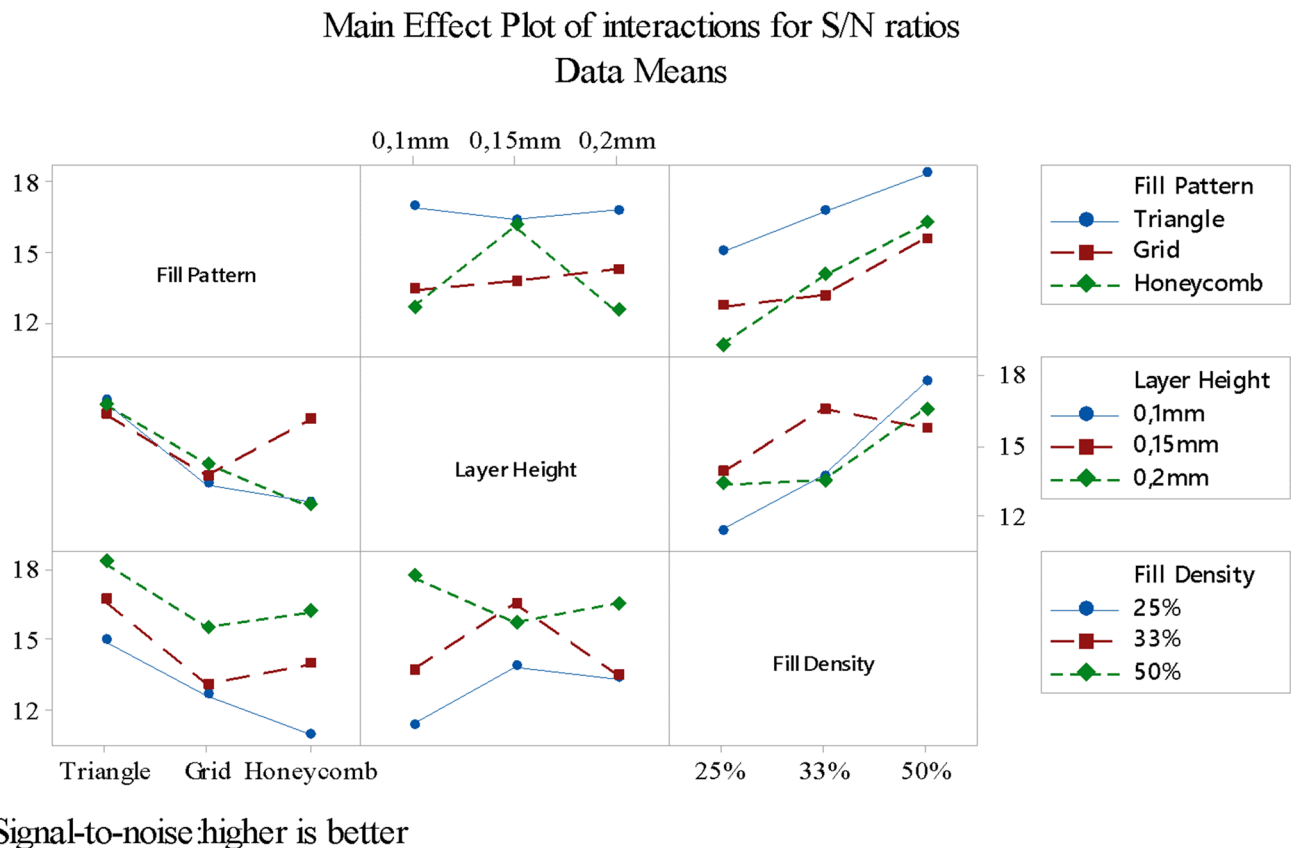
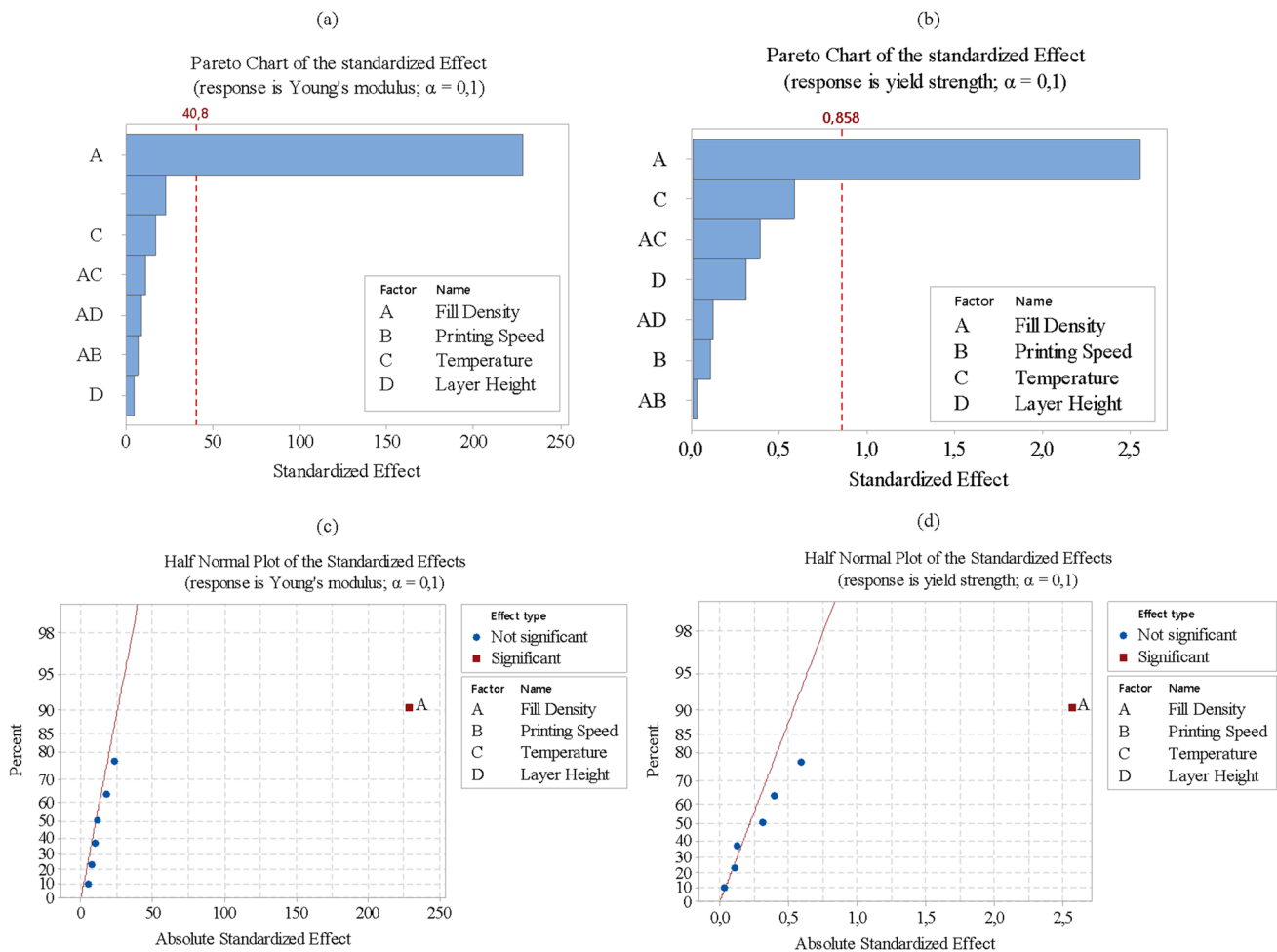


Fig. 9 Main effects plot for S/N ratios



**Fig. 10** Effect plots for analyze factorial design: (a) Pareto chart for Young's modulus and (b) Pareto chart for yield strength. Half normal probability plot of the effects for (c) Young modulus and (d) yield strength

**Table 3** Factors and control levels used for fractional factorial designs ( $2^{4-1}$ )

Parameters	Code	Level		Unit
		1	2	
Infill density	A	25	50	%
Printing velocity	B	1000	3000	mm/min
Temperature	C	210	215	°C
Layer height	D	0.1	0.2	mm

hypothesis that the effect is 0. A reference line calculated at 40.8 and 0.858 for both Young's modulus and yield strength, respectively, indicates which effects are statistically significant. The reference line for statistical significance depends on the significance level denoted by  $\alpha$ , which is choosing equal to 0.1 in current model.

The plots in Fig. 10a and b indicate that the infill density factor have a significant effect on both Young's modulus and

yield strength since it is the only factor that intersects both the reference lines. However, all other factors and interactions do not show main effect and were considered as negligible.

Using the half normal probability plot of the effects permits to examine which factors are important and which are not on one plot. Figure 10c and d show the half normal probability plot of the effects. Effects that are further from 0 are statistically significant. On this plot, only the infill density parameter is to be retained as significant factor at the  $\alpha = 0.1$  level.

## 4 Conclusions

Understanding the relation between process parameters and mechanical behavior of FDM<sup>TM</sup>/FFF parts is very important if the objective is to minimize the weight and obtain a material with controlled properties. This study focused on the influence of different printing parameters over the

elastic mechanical properties of PLA material by considering their individual and/or interaction effects. Based on the literature reviews, the selected parameters in this work are (i) infill pattern, (ii) layer height, (iii) infill density, (iv) printing velocity, (v) raster orientation, (vi) outline overlap, and (vii) extruder temperature. The elastic mechanical properties that are object are Young's modulus and Yield strength. To reduce experimental runs, the  $L_{27}$  Taguchi orthogonal array supplemented by a two-level fractional factorial design with four-factor ( $2^{4-1}$ ) approach was used. Based on experimental results obtained in this work, the following conclusions can be drawn:

- The minimum and maximum values obtained for apparent Young's modulus of all the different permutations of the  $L_{27}$  array were 248 MPa and 796 MPa, respectively, whereas for the yield strength were 2.04 MPa and 9.49 MPa, respectively.
- It was shown that for both apparent Young's modulus and yield strength, the most significant parameter are (F3) infill density, (F1) infill pattern, (F4) printing speed, and (F5) printing orientation. For apparent Young's modulus, the contribution of each factor was ~36% for (F3) infill density, ~29.2% for (F1) infill pattern, ~14% for printing velocity, and ~11.7% for printing orientation, whereas for the yield strength, the contribution was 27.6%, 21.5%, 16%, and 13.4% for (F3) infill density, (F1) infill pattern, (F5) printing orientation, and (F4) printing speed, respectively. The remaining factors (F2) layer height, (F6) outline overlap, and (F7) temperature were less significant.
- The optimum combination of factors for higher Young's was meeting at (F3) infill density, 50%; (F2) infill pattern, triangle; (F4) printing speed, 3 m/min; (F5) printing orientation, 45°; (F2) layer height, 0.1 mm; (F7) temperature, 210 °C; and (F6) outline overlap, 30%, whereas for the yield strength, the difference was observed in the two last parameters, which is considered without a significant effect: (F7) temperature, 205 °C, and (F6) outline overlap, 20%.
- The fractional factorial design method confirms that the most important factor is infill density. The remaining factors (B) velocity, (C) temperature, and (D) layer height with three interactions AB, AC, and AD show no significant effect.

The methodology applied in this paper could be readily applied to different 3D process technologies. This research work could be further developed to propose a meta model to help designers to obtain either tailor-made or a robust mechanical property with minimum variation and uncertainty. Because that the FDM<sup>TM</sup>/FFF printing parts are highly orthotropic materials, it is important to verify that the mechanical properties of specimens are independent of

the geometry (scalability effects). Future research goes in these directions.

**Funding** The authors received no financial support for the research, authorship, and/or publication of this article.

**Data availability** The data that support the findings of this study are available from the corresponding author, upon reasonable request.

**Code availability** Not applicable.

## Declarations

**Conflict of interest** The authors declare no competing interests.

## References

1. ASTM F2792–12a. Standard Terminology for Additive Manufacturing Technologies. vol. 10.04.
2. Terekhina S, Tarasova T, Egorov S, Skorniyakov I, Guillaumat L, Hattali ML (2021) Flexural quasi-static and fatigue behaviours of fused filament deposited PA6 and PA12 polymers. *Int J Adv Manuf Tech*. <https://doi.org/10.1007/s00170-021-07223-y>
3. Safai L, Cuellar JS, Smit G, Zadpoor AA (2019) A review of the fatigue behavior of 3D printed polymers. *Adv Manuf* 28:87–97. <https://doi.org/10.1016/j.ADDMA.2019.03.023>
4. Ziemian S, Okwara M, Ziemian CW (2015) Tensile and fatigue behavior of layered acrylonitrile butadiene styrene. *Rapid Prototyp J* 21(3):270–278
5. Ziemian C, Ziemian R, Haile K (2016) Characterization of stiffness degradation caused by fatigue damage of additive manufactured parts. *Mater Des* 109 (Supplement C): 209 – 218. <https://doi.org/10.1016/j.matdes>
6. Popescu D, Zapciu A, Amza C, Baciuc F, Marinescu R (2018) FDM process parameters influence over the mechanical properties of polymer specimens: A review. *Polym Testing* 69:157–166. <https://doi.org/10.1016/j.polymertesting.2018.05.020>
7. Harris M, Potgieter J, Archer R, Arif KM (2019) Effect of Material and Process Specific Factors on the Strength of Printed Parts in Fused Filament Fabrication: A Review of Recent Developments. *Materials*, 22;12(10):1664. <https://doi.org/10.3390/ma12101664>.
8. Ahn SH, Montero M, Odell D, Roundy S, Wright PK (2002) Anisotropic material properties of fused deposition modeling ABS. *Rapid Prototyp J* 8(4):248–257. <https://doi.org/10.1108/13552540210441166>
9. Chin Ang K, Fai Leong K, Kai Chua C, Chandrasekaran M (2006) A investigation of the mechanical properties and porosity relationships in fused deposition modelling fabricated porous structures. *Rapid Prototyp J* 12(2):100–105. <https://doi.org/10.1108/13552540610652447>
10. Onwubolu GC, Rayegani F (2014) Characterization and Optimization of Mechanical Properties of ABS Parts Manufactured by the Fused Deposition Modelling Process. *Int. J. Manuf. Eng*. <https://doi.org/10.1155/2014/598531>.
11. Anitha R, Arunachalam S, Radhakrishnan P (2001) Critical parameters influencing the quality of prototypes in fused deposition modelling. *J Mater Process Technol* 118(1–3):385–388. [https://doi.org/10.1016/S0924-0136\(01\)00980-3](https://doi.org/10.1016/S0924-0136(01)00980-3)



12. Chohan JS, Singh R (2016) Enhancing dimensional accuracy of FDM based biomedical implant replicas by statistically controlled vapor smoothing process. *Prog Addit Manuf* 1(1):105–113. <https://doi.org/10.1007/s40964-016-0009-4>
13. Mahmoudian M, Poursattar Marjani A, Hasanzadeh R et al (2020) Optimization of mechanical properties of in situ polymerized poly(methyl methacrylate)/alumina nanoparticles nanocomposites using Taguchi approach. *Polym Bull* 77:2837–2854. <https://doi.org/10.1007/s00289-019-02885-x>
14. Nancharaiha T (2011) Optimization of Process Parameters in FDM Process Using Design of Experiments. *Optimize* 2(1):100–102
15. Jiang J, Ma Y (2020) Path planning strategies to optimize accuracy, quality, built time and material use in additive manufacturing: A review. *Micromachines* 11(7), 633; <https://doi.org/10.3390/mi11070633>
16. Boschetto A, Giordano V, Veniali F (2013) Surface roughness prediction in fused deposition modelling by neural networks. *Int J Adv Manuf Technol* 67:2727–2742. <https://doi.org/10.1007/s00170-012-4687-x>
17. Vahabli E, Rahmati S (2016) Application of an RBF neural network for FDM parts' surface roughness prediction for enhancing surface quality. *Int J Precis Eng Manuf* 17:1589–1603. <https://doi.org/10.1007/s12541-016-0185-7>
18. Jiang J, Hu G, Li X, Xu X, Zheng P, Stringer J (2019) Analysis and prediction of printable bridge length in fused deposition modelling based on back propagation neural network. *Virtual and physical prototyping* 14(3):253–266. <https://doi.org/10.1080/17452759.2019-0010>
19. Sahu RK, Mahapatra SS, Sood AK (2013) A Study on Dimensional Accuracy of Fused Deposition Modeling (FDM) Processed Parts using Fuzzy Logic. *Journal for Manufacturing Science & Production* 13(3):183–197. <https://doi.org/10.1515/jmsp-2013-0010>
20. Rodriguez JF, Thomas JP, Renaud JE (2001) Mechanical behavior of acrylonitrile butadiene styrene (ABS) fused deposition materials. *Experimental Investigation. Rapid Prototyp. J.* 7 (3)148–158. <https://doi.org/10.1108/13552540110395547>
21. Sun Q, Rizvi GM, Bellehumeur CT, Gu P (2008) Effect of processing conditions on the bonding quality of FDM polymer filaments. *Rapid Prototyp J* 14(2):72–80. <https://doi.org/10.1108/13552540810862028>
22. Terekhina S, Egorov S, Guillaumat L, Tarasova T, Hattali ML (2020) On the difference in material structure and fatigue properties of polyamide specimens produced by fused filament fabrication and selective laser sintering. *Int J Adv Manuf Tech.* <https://doi.org/10.1007/s00170-020-06026-x>
23. Terekhina S, Skorniyakov I, Egorov S, Guillaumat L, Tarasova T, Hattali ML (2020) The effect of build orientation on both flexural quasi-static and fatigue behaviors of filament deposited PA6 polymer. *Int J fatigue* 140:105825. <https://doi.org/10.1016/j.ijfatigue.2020.105825>
24. Wang C, Lin T, Hu S (2007) Optimizing the rapid prototyping process by integrating the Taguchi method with the Gray relational analysis. *Rapid Prototyping Journal* 13(5):304–315. <https://doi.org/10.1108/13552540710824814>
25. Fatimatuzahraa AW, Farahaina B Yusoff WAY (2011) The effect of employing different raster orientations on the mechanical properties and microstructure of Fused Deposition Modeling parts. *Business, Engineering and Industrial Applications (ISBEIA). IEEE Symposium.* 22–27. <https://doi.org/10.1109/ISBEIA.2011.6088811>
26. Maurya NK, Rastogi V, Singh P (2020) An overview of mechanical properties and form error for rapid prototyping, *CIRP Journal of Manufacturing Science and Technology. Part A* 29:53–70. <https://doi.org/10.1016/j.cirpj.2020.02.003>
27. Rankouhi B, Javadpour S, Delfanian F, Letcher T (2016) Failure analysis and mechanical characterization of 3D printed ABS with respect to layer thickness and orientation. *J Fail Anal Prev* 16:467–481. <https://doi.org/10.1007/s11668-016-0113-2>
28. Lechter T, Rankouhi B, Javadpour S (2015) Experimental study of mechanical properties of additively Manufactured abs plastic as a function of layer parameters. *ASME 2015 International Mechanical Engineering Congress and Exposition. 2A: Advanced Manufacturing, Houston, Texas*
29. Tymrak BM, Kreiger M, Pearce LM (2014) Mechanical properties of components fabricated with open-source 3-D printers under realistic environmental conditions. *Mater Des* 58:242–246. <https://doi.org/10.1016/j.matdes.2014.02.038>
30. Es-Said O, Foyos J, Noorani R, Mendelson M, Marloth R, Pregar B (2000) Effect of layer orientation on mechanical properties of rapid prototyped samples. *Mater Manuf Processes* 15(1):107–122. <https://doi.org/10.1080/10426910008912976>
31. Chacon J, Caminero M, García-Plaza E, Núñez P (2017) Additive manufacturing of PLA structures using fused deposition modelling: effect of process parameters on mechanical properties and their optimal selection. *Mater Des* 124:143–157. <https://doi.org/10.1016/j.matdes.2017.03.065>
32. Li H, Wang T, Sun J, Yu Z (2018) The effect of process parameters in fused deposition modelling on bonding degree and mechanical properties. *Rapid Prototyp J* 24(1):80–92. <https://doi.org/10.1108/RPJ-06-2016-0090>
33. Torres J, Cole M, Owji A, DeMastry Z, Gordon AP (2016) An approach for mechanical property optimization of fused deposition modeling with polylactic acid via design of experiments. *Rapid Prototyp J* 22(2):387–404. <https://doi.org/10.1108/RPJ-07-2014-0083>
34. Xiaoyong S, Liangcheng C, Honglin M, Peng G, Zhanwei B, Cheng L (2017) Experimental analysis of high temperature PEEK materials on 3D printing test. *9th International Conference on Measuring Technology and Mechatronics Automation*, pp 13–16
35. Behzadnasab M, Yousefi A (2016) Effects of 3D printer nozzle head temperature on the physical and mechanical properties of PLA based product. *12th International seminar on polymer science and technology effects of 3D printer nozzle head temperature on the physical and mechanical properties of PLA based product*, pp 3–5, November
36. Thompson MK, Moroni G, Vaneker T, Fadel G, Campbell RI, Gibson I, Bernard A, Schulz J, Graf P, Ahuja B, Martina F (2016) Design for additive manufacturing: trends, opportunities, considerations, and constraints. *CIRP Ann Manuf Technol* 65:737–760
37. Quinsat Y, Lartigue C, Brown CA, Hattali L (2018) Characterization of surface topography of 3D printed parts by multi-scale analysis. *Int J Interact Des Manuf* 12:1007–1014. <https://doi.org/10.1007/s12008-017-0433-9>
38. Azdast T, Hasanzadeh R (2021) Polylactide scaffold fabrication using a novel combination technique of fused deposition modeling and batch foaming: dimensional accuracy and structural properties. *Int J Adv Manuf Technol* 114:1309–1321. <https://doi.org/10.1007/s00170-021-06915-9>
39. Fernandes J, Deus AM, Reis L, Vaz MF, Leite M (2018) Study of the influence of 3D printing parameters on the mechanical properties of PLA. *Proceedings of the 3rd International Conference on Progress in Additive Manufacturing (Pro-AM 2018)*, pp 547–552. <https://doi.org/10.25341/D4988C>
40. Deng X, Zeng Z, Peng B, Yan S, Ke W (2018) Mechanical properties optimization of poly-ether-ether-ketone via fused deposition modeling. *Materials* 11:216
41. Rinanto A, Nugroho A, Prasetyo H, Pujiyanto E (2018) Simultaneous optimization of tensile strength, energy consumption and processing time on FDM process using taguchi and PCR-TOPSIS. In:



- Proceedings of the 2018 4th International Conference on Science and Technology (ICST), Yogyakarta, Indonesia, 7–8 August 2018; pp. 1–5
42. Alafaghani, A, Qattawi, A, Alrawi B, Guzman A (2017) Experimental optimization of fused deposition modelling processing parameters: a design for manufacturing approach. *Procedia Manuf* 791–803. <https://doi.org/10.1016/j.promfg.2017.07.079>
  43. Aw Y, Yeoh C, Idris M, Teh P, Hamzah K, Sazali S (2018) Effect of printing parameters on tensile, dynamic mechanical, and thermoelectric properties of FDM 3D printed CABS/ZnO composites. *Materials* 11:466
  44. Harpool TD, Alarifi IM, Alshammari BA, Aabid A, Baig M, Malik RA, Mohamed Sayed A, Asmatulu R, EL-Bagory TMAA, (2021) Evaluation of the Infill Design on the Tensile Response of 3D Printed Polylactic Acid Polymer. *Materials* 14(9):2195. <https://doi.org/10.3390/ma14092195>
  45. ASTM D638 - 10. Standard Test Method for Tensile Properties of Plastics. D20.10. Ed. West Conshohocken. PA: ASTM International. 2011. [Online]. Available: [www.astm.org](http://www.astm.org)
  46. BS EN ISO 527–2: 1996 Plastics - Determination of tensile properties - Part 2: Test conditions for moulding and extrusion plastics
  47. Taguchi G, Chowdhury S, Wu Y (2005) Taguchi's quality engineering handbook. <https://doi.org/10.1002/9780470258354>
  48. Wang K, Xie X, Wang J, Zhao A, Peng Y, Rao Y (2020) Effects of infill characteristics and strain rate on the deformation and failure properties of additively manufactured polyamide-based composite structures. *Results Phys* 18. <https://doi.org/10.1016/j.rinp.2020.103346>
  49. Lubombo C, Huneault M (2018) Effect of Infill Patterns on the Mechanical Performance of Lightweight 3D-Printed Cellular PLA Parts. *Materials Today Communications*. <https://doi.org/10.1016/j.mtcomm.2018.09.017>

**Publisher's note** Springer Nature remains neutral with regard to jurisdictional claims in published maps and institutional affiliations.